A homogenization approach for large-scale flows interacting with fine-grained poroelastic media

Giuseppe A. Zampogna*, Ph.D. University of Genova, March 2016, supervisor: Prof. A. Bottaro
*DICCA, Via Montallegro 1, 16145, Genova, IT. Email: giuseppe.zampogna@edu.unige.it Phone: +3901853532560

Abstract:
In Nature, fluid-structure interactions are often characterized by separation of scales, due to the presence of small-scale roughness or deformable irregularities present on macroscopic surfaces. It is the case, for instance, of the scales which cover the wings of the butterflies or the shark's skin, the barbules which characterize the owl's feathers or the microscopic protrusions present on the surface of lotus' leaves. A way to bypass the complexity of fine-grained numerical simulations is to consider macroscopic approaches which disregard the microscopic properties of the structure aside from the presence of *effective* tensorial properties which results from the solution of microscopic problems. This homogenization perspective is taken in the author's thesis, where particular attention is paid also to regimes in which inertia within the pores is not negligible.

Keywords: Biomimetics, anisotropic poroelasticity, effective approach, homogenization.

Nature's strategy

Nature is never regular. Lines are not straight, surfaces are not smooth and the fact that Earth is a geoid is only an approximation. The degree of irregularity is a matter of perspective.

To observe things from a microscopic point of view necessarily leads to the conclusions above, which complicate issues when dealing, for instance, with fluid-structure interaction phenomena. If we imagine to have to simulate the flow over a surface characterized by elastic, microstructured protrusions, we need to calculate the fluid pressure and velocity in each interstice between the structures, plus the deformation of each structure, taking into account how fluid and solid interact. How convenient would it be to transform an irregular surface into a homogeneous region ruled by modified macroscopic equations, without any loss of information relative to the microstructure? This is the scope of the present thesis, where a multiple scale approach is adopted to yield macroscopic equations which govern the interaction between a pure fluid region (F) and a homogenized, poroelastic medium (H).

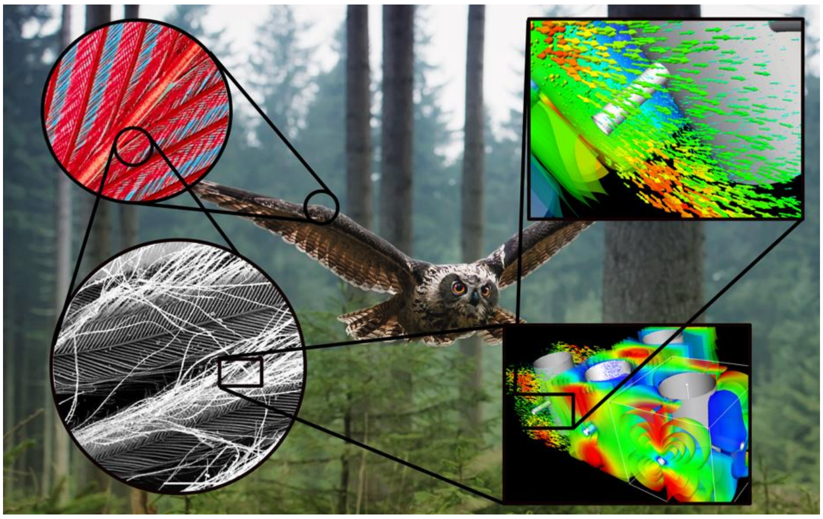

Figure 1: *The flight of an owl is considered as a case to illustrate multiscale phenomena. A macroscopic dimension (e.g. the wingspan) is compared to the size of the barbules of the feathers (μm). The owl's feathers are microscopically modeled as a poroelastic medium. The insets on the left show the feathers at two different scales, while on the right there are different visualizations of the flow field near the feathers. In the present work microscopic problems are solved to extract effective tensors which define the macroscopic behaviour of the flow.*

An *effective* set of equations

A homogenization, multiple scale technique (cf. [1, 2] for a more extensive explanation) is used to obtain the *effective* or macroscopic model. The unknowns are the fluid velocity $\boldsymbol{u}$, the pressure p and the displacement of the structure $\boldsymbol{v}$; they must be intended as quantities which vary only over the macroscale, since they are averaged as explained in the caption of fig. 2. The *effective* balance equations on H are:

$$\begin{cases} (1-\vartheta)\ddot{\boldsymbol{v}} = \nabla\cdot[\boldsymbol{\mathcal{C}} : \boldsymbol{\varepsilon}(\boldsymbol{v}) - \alpha \boldsymbol{I} p], & (1a)\\ \langle\nabla\cdot\boldsymbol{\eta}\rangle\dot{p} - \nabla\cdot\boldsymbol{\mathcal{K}}\cdot\nabla p = \langle\nabla\cdot\boldsymbol{\chi}\rangle : \boldsymbol{\varepsilon}(\dot{\boldsymbol{v}}) - \vartheta\nabla\cdot\dot{\boldsymbol{v}}, & (1b)\\ \langle\boldsymbol{u}\rangle - \vartheta\,\dot{\boldsymbol{v}} = -\boldsymbol{\mathcal{K}}\cdot\nabla p, & (1c)\end{cases}$$

where $\boldsymbol{\mathcal{K}}$, $\boldsymbol{\mathcal{C}}$, $\boldsymbol{\alpha}$, $\boldsymbol{\eta}$, $\boldsymbol{\chi}$ are tensors deduced from the solution of problems over V, defined in fig. 2. The porosity ϑ is defined as the void fraction within V; $(1a)$ is the governing equation for the displacement; $(1b)$ links the fluid pressure to the displacement and $(1c)$, a generalization of Darcy's law, allows to calculate the fluid velocity once p and $\boldsymbol{v}$ are found. As the name of the technique suggests, the mathematical hypotheses on which system (1) is based, are valid only in a homogeneous region, "far" from the macroscopic boundaries of the poroelastic domain.

Suitable interface conditions are needed to couple model (1) with the Navier-Stokes equations which apply in the free-fluid region. A study of the possible interface conditions has been done in [1, 2]; the set of conditions appropriate for the poroelastic case are:

$$\begin{cases} \langle \boldsymbol{u} \rangle^H = \boldsymbol{u}^F, & (2a) \\ \langle \boldsymbol{\Sigma}^H \rangle \cdot \boldsymbol{n} = \boldsymbol{\sigma}^F \cdot \boldsymbol{n}, & (2b) \\ (\boldsymbol{n} \cdot \boldsymbol{\mathcal{K}}) \cdot \nabla p^H = \dfrac{\mathcal{K}^I}{d^I} P^{F-H}, & (2c) \end{cases}$$

where the superscripts F or H denote the region we are in. While $(2a, 2b)$ are classical and commonly accepted conditions for $\boldsymbol{u}$ and $\boldsymbol{v}$, [3] has shown by DNS the presence of a pressure jump. Here the jump is quantified by equation $(2c)$ as in [4]: the normal to the interface pressure gradient inside H is proportional to the pressure jump ($P^{F\text{-}H}$) between the F-H interface I, considered as a membrane of isotropic permeability $\mathcal{K}^I$ and thickness d^I.

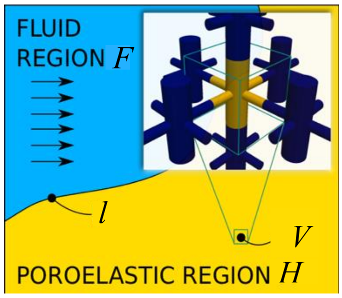

Figure 2: *In the present problem, two macroscopic regions can be identified: a pure fluid region and a region occupied by a poroelastic medium. If the solid skeleton is periodically micro-structured, in the poroelastic medium we can identify an elementary cell V, divided into two phases: the solid V_S and the fluid V_F. The hypothesis needed to apply homogenization is that $\epsilon = \frac{l}{L} \ll 1$, where l and L are, respectively, the characteristic macroscopic and microscopic dimensions. This leads us to the definition of an average over V, denoted with $\langle\cdot\rangle$, thanks to which the unknowns, once averaged, are defined on the H domain where there is no distinction between V_S and V_F. Different flow regimes can be identified on the basis of $Re = Ul/\nu$, with ν the fluid viscosity and U the reference macroscale velocity.*

Large-Re flow in a canopy

In order to test if the way to calculate the permeability for Re larger than $\mathcal{O}(\epsilon)$ works reasonably well (the procedure is explained in the inset below), the present model has been compared with experiments in [6], where a turbulent flow through and near a canopy made of vertical rigid cylinders is simulated. Assuming a constant mixing length model [5], we find an analytical form for the velocity in the pure fluid region. In the canopy, eq. (1c) is valid (the term $\vartheta\, \dot{\boldsymbol{v}}$ disappears since the cylinders are rigid). The entire profile can be seen in fig. 3, plotted against experimental results. A posteriori evaluation of $\boldsymbol{\mathcal{K}}$ (deduced from the measurements of $\boldsymbol{u}$ and ∇p by inverting $1c$) shows that model (3) gives results in acceptable agreement with the literature (cf. figs. 4 and 5).

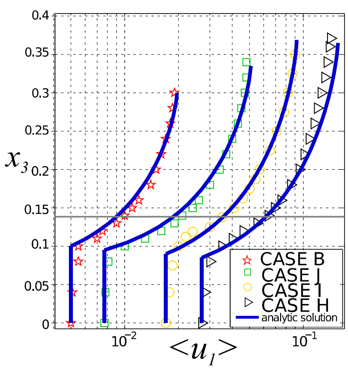

Figure 3: *Full profiles of $\langle u_1 \rangle$ for four different experiments (using the notations in [6]). The symbols represent the experiments, the solid lines the analytical solution computed in [5].*

Poroelastic coatings

While the first application presented was a steady case related to hydrodynamics, an unsteady application in aerodynamics is proposed next. A channel flow, forced by an oscillating pressure gradient, is studied (cf. [1, 8] for details). The lower half of the channel is covered by a poroelastic layer of polyurethane foam, whose microstructure is represented in fig. 7 together with some components of $\boldsymbol{\chi}$. The disturbances generated by the medium are studied. Fig. 8 shows the vortical structures which arise in the interfacial zone and influence a non-negligible part of the fluid domain.

The *effective* permeability tensor $\mathcal{K}$

The *effective* permeability represents the property of a porous medium to be permeated by a fluid. It is a canonical physical quantity postulated in [7]. For $Re = O(\epsilon)$, it is found solving a Stokes problem over V_F. In case of larger Re, $\boldsymbol{\mathcal{K}}$ an intrinsic property of the medium, but depends on the flow regime, so that the Stokes problem is forced by a term which depends on Re:

$$\begin{cases} \nabla \boldsymbol{A} - \nabla^2 \boldsymbol{K} = \boldsymbol{I} - Re\boldsymbol{U} \cdot \nabla \boldsymbol{K}, \\ \nabla \cdot \boldsymbol{K} = 0, \end{cases} \qquad (3)$$

(cf. [1] for the mathematical development). The macroscopic behavior of $\boldsymbol{\mathcal{K}} = \langle \boldsymbol{K} \rangle$ is summarized by figs. 4 and 5. They show that is an increasing function of the porosity and a decreasing function of $Re\boldsymbol{U}$, respectively. Since $\boldsymbol{U}$ is a macroscopic mean velocity in H, an iterative procedure, between the macro and microscopic solution, must be performed to find $\boldsymbol{K}$ (cf. [1]).

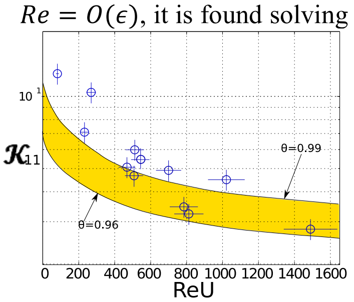

Figure 4: $\boldsymbol{\mathcal{K}_{11}}$ *in case of large-Re, for ϑ=0.96-0.99. The band is determined with eq. (3); the blue circles, with respective error bars, are deduced by experiments [6].*

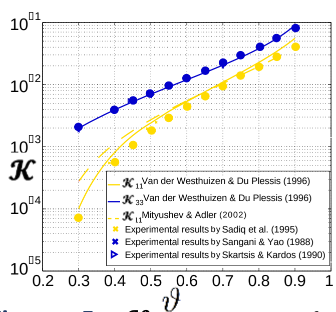

Figure 5: $\boldsymbol{\mathcal{K}_{ii}}$ *in case of negligible Re, for ϑ=0.3-0.9. Blue and yellow bullets are the solutions of a Stokes problem over V_F.*

Effective quantities related to the solid

Homogenization gives *effective* tensors which allow to transfer the microscopic behavior of the structure to the macroscopic scale. For the solid model, we solve for a third order tensor $\boldsymbol{\chi}$ and a vector $\boldsymbol{\eta}$, whose description can be found in [1, 8]. These quantities allow to define the *effective* porosity $\boldsymbol{\alpha}$, which can be seen as a modified porosity because of fluid pressure force: $\boldsymbol{\alpha} = \vartheta \boldsymbol{I} + \langle \boldsymbol{C}:\boldsymbol{\varepsilon}(\boldsymbol{\eta})\rangle$, with $\boldsymbol{C}$ the microscopic elasticity tensor determined by the type of material we are considering. The *effective* elasticity tensor $\boldsymbol{\mathcal{C}}$ characterizes the elastic behavior of the solid not only on the basis of the material but also taking into account the geometrical shape of the structure. Fig. 7 shows the non-zero entries of $\boldsymbol{\mathcal{C}}$:

$$\boldsymbol{\mathcal{C}} = \langle \boldsymbol{C}:\boldsymbol{\varepsilon}(\boldsymbol{\chi})\rangle + \langle \boldsymbol{C}\rangle.$$

for varying $\vartheta \in (0.3,1)$ and the chosen shape (right) of the microstructure.

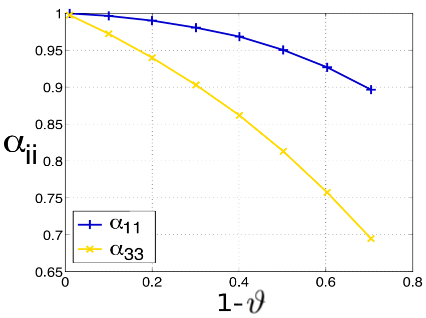

Figure 6: *Non-zero components of* $\boldsymbol{\alpha}$ *for* ϑ*=0.3-1.*

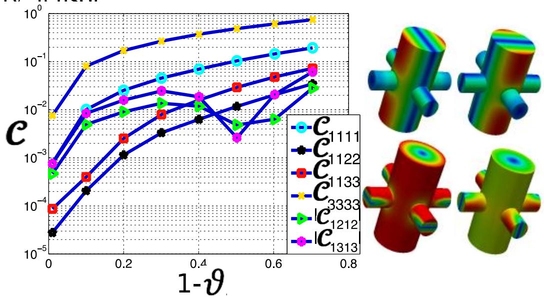

Figure 7: *Entries of* $\boldsymbol{\mathcal{C}}$*. On the right, some components of* $\boldsymbol{\chi}$ *over* V_S *are shown (*$|\chi_{11}|, |\chi_{22}|, |\chi_{12}|, |\chi_{33}|$ *clockwise from top left).*

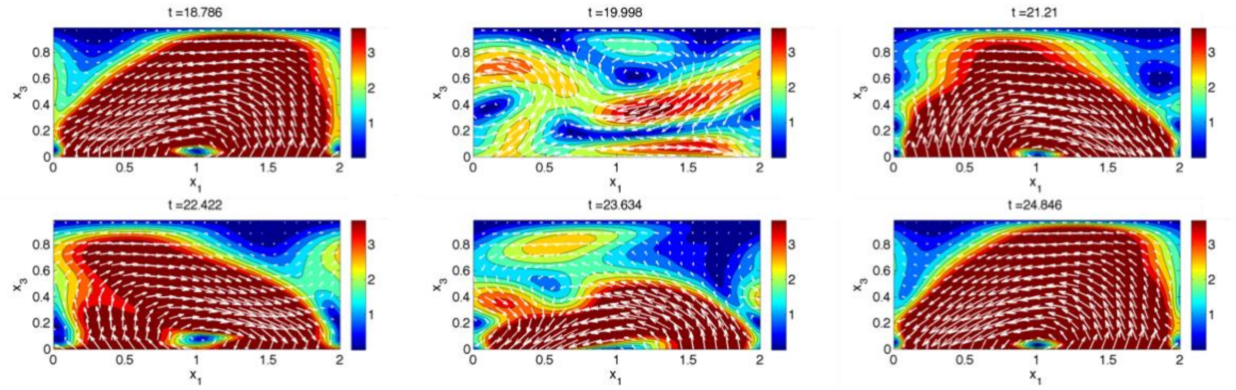

Figure 8: *Disturbance velocity (white arrows) and kinetic energy (colors) of the flow due to the presence of a homogeneous medium positioned in the lower half of the channel (for* $x_3 \in (-1,0)$*). Only the pure fluid region F is shown, for six different instants of a periodic cycle. Periodic boundary conditions are enforced along* x_1*.*

Conclusions

The present thesis has focussed on finding *effective* properties for macroscopic models of flows through anisotropic porous and poroelastic media, from the numerical solution of microscopic equations, including the effect of inertia. Validation of the coupled problem, including a pure fluid region and a homogenized medium, have been carried out comparing results to DNS and to experimental data from the literature. Different kinds of interface conditions have been considered, highlighting the pros and cons of each.

Scientific output

The Ph.D. work has resulted in two journal papers (refs. [2, 5]) and one paper under review (ref. [8]), a conference proceeding (AIMETA XXII) and four technical reports for the European project ACP2-GA-2013-334954-PEL-SKIN. One more paper (ref. [9]) and two conference proceedings (AIMETA XXI, ETC14) have been published on a related topic and a last paper is in the final stages before submission (ref. [10]). The author's thesis has been awarded the "Best Ph.D Thesis" prize in fluid dynamics by the University of Genova.

REFERENCES:

[1] Zampogna, G.A., 2016. Flows over and through poroelastic media: a homogenized approach. *Ph.D. Thesis*, Genova.

[2] Zampogna, G.A. & Bottaro, A., 2016. Fluid flow over and through a bundle of rigid fibres. *Journal of Fluid Mechanics*, **792**, 1-33.

[3] Carraro, T. et al., 2013. Pressure jump interface law for the Stokes–Darcy coupling: confirmation by direct numerical simulations. *Journal of Fluid Mechanics*, **732**, 510-536.

[4] Gopinath, A. & Mahadevan, L., 2010. Elastohydrodynamics of wet bristles, carpets and brushes. *Proceedings of the Royal Society,* **467**, 1665-1685.

[5] Zampogna, G.A. et al., 2016. Instability of canopy flows. *Water Resource Research*. DOI:10.1002/2016WR018915.

[6] Ghisalberti, A. & Nepf, H., 2004. The limited growth of vegetated shear layers. *Water Resource Research*, **40** (7), 1-12.

[7] Darcy, H., 1856. Les fontaines publique de la ville de Dijon, *Victor Dalmont Editeur*, Paris.

[8] Zampogna, G.A. & Bottaro, A., 2016. The PELskin project: Part III. *Meccanica*, submitted.

[9] Wedin, H. et al., 2014. Unstable flow structures in the Blasius boundary layer. *The European Physical Journal,* **37**,34.

[10] Zampogna, G.A. et al. 2016. Flows through poroelastic media. *Journal of Fluid Mechanics*, to be submitted.